International Journal of Applied Engineering Research ISSN 0973-4562 Volume 13, Number 7 (2018) pp. 4652-4662

MHD Convective Flow of Second Grade Fluid through Porous Medium between Two Vertical Plates with Mass Transfer

G.Sudarsan Reddy[1*] and G.Viswanatha Reddy[2]

[1]*Research Scholar, Department of Mathematics, Rayalaseema University, Kurnool-518007, Andhra Pradesh, India.*

[2]*Associate Professor, Department of Mathematics, Sri Venkateswara University, Tirupathi-517502, Andhra Pradesh, India.*

Abstract

In this chapter, an investigation of the heat and mass transfer on the flow of an oscillatory convective MHD viscous incompressible, radiating and electrically conducting second grade fluid in a vertical porous rotating channel in slip flow regime is carried out. The fluid is assumed to be gray, absorbing and emitting radiation out in non scattering medium. The MHD flow is assumed to be laminar and fully developed. A closed form solutions of the equations governing the flow are obtained for the velocity and temperature distributions making use of regular perturbation technique. The velocity, temperature and concentration profiles are discussed through graphically as well as skin friction coefficient, Nusselt number and Sherwood number are evaluated numerically and presented in the form of tables and discussed for different values of governing flow parameters.

Keywords: Hall Effect, radiating fluid, MHD oscillatory flow, rotating channel, slip flow regime.

Nomenclature:

(u, v)	the velocity components along x and y directions
p	the modified pressure
t	time
C_p	Specific heat
B_0	electromagnetic induction
g	Acceleration due to gravity
K_1	thermal conductivity
k	permeability of the porous medium
Q_0	Heat absorption
T	temperature of the fluid
f_1	Maxwell's reflection co-efficient
μ	Co-efficient of viscosity
L	mean free path
T_0	mean temperature
w_0	suction velocity
q_1	radiative heat
q	Complex velocity
M	Hartmann number
K	Permeability parameter
S	second grade fluid parameter
R	Rotation parameter
Gr	thermal Grashof number
Pr	Prandtl number
D	the molecular diffusivity
K_c	the chemical reaction parameter
C	concentration
C_0	mean concentration
Q_1	Radiation absorption

Greek symbols

α	the mean variation absorption coefficient
α_1	normal stress moduli
θ	Dimension less temperature
ϕ	Dimension less concentration
Ω	Angular velocity
σ	Electrical conductivity of the fluid
ρ	Density of the fluid
ν	Kinematic viscosity
ω	the frequency of oscillation
β	The coefficient of volume expansion
β_c	The coefficient of volume expansion with concentration

INTRODUCTION

During the past several decades, convective flow through porous media has been a subject of considerable research interest of a large number of scholars due to its diverse engineering applications. These applications include, but are not limited to, for example heat exchangers in high heat flux applications such as electronic equipment, insulation of the heated body, thermal energy storage and sensible heat storage beds, drying process (wood and food products), air conditioning and filtration process. During the last decades, several researchers studied free convection heat and mass transfer in a porous medium [1e3]. Mass transfer effects on flow past an accelerated vertical plate has already been well studied [4,5]. Furthermore, the problem of heat and mass transfer of nonNewtonian fluids in porous media has been a subject of interest in many research projects [6e10]. In recent years, considerable attention has been devoted to the study of magetohydrodynamics (MHD) flow and heat. In addition to useful features of MHD flows, such studies can be helpful in prediction of the effects of magnetic intrusions. Raptis and Singh [11] studied MHD free convection flow past an accelerated vertical plate. Taza Gul et al. [12] studied heat transfer of MHD thin film flow of an unsteady second grade fluid past a vertical oscillating belt by analytical techniques. In recent years there has been a growing interest in studying the combined application of MHD flow and porous media. Since the use of magnetic field can influence the heat generation/absorption process in electrically conducting fluid flows, the rate of cooling in many metallurgical processes and consequently the desired properties of the end product can be controlled. Furthermore, the influence of magnetic field on boundary layer flows has brought about its application in geothermal energy recovery, oil extraction and thermal insulations. Abdulhameed et al. [13] obtained exact solution for an unsteady two-dimensional MHD flow of incompressible viscous fluid over a flat plate with wall transpiration embedded in a porous medium. Aldoss et al. [14] investigated combined free and forced convection flow from a vertical plate embedded in a porous medium in the presence of a magnetic field. Chamkha [15] considered a plate embedded in a uniform porous medium which moves with a constant velocity in the flow direction in the presence of a transverse magnetic field. Reddy [16] studied radiation effects on MHD natural convection flow along a vertical cylinder embedded in a porous medium with variable surface temperature and concentration. Also, Olajuwon et al. [17] investigated the effect of thermal radiation and Hall current on MHD flow of a viscoelastic micropolar fluid through a porous medium. Furthermore, unsteady MHD flow in porous media has been studied by several researchers [18-20]. Combined buoyancy-generated heat and mass transfer are characterized by highly non-linear coupled partial differential equations which are required to be solved by numerical computations. In recent years different researchers have used and discussed various numerical modeling techniques [21-25]. Recently, Krishna and Swarnalathamma [26] discussed the peristaltic MHD flow of an incompressible and electrically conducting Williamson fluid in a symmetric planar channel with heat and mass transfer under the effect of inclined magnetic field. Swarnalathamma and Krishna [27] discussed the theoretical and computational study of peristaltic hemodynamic flow of couple stress fluids through a porous medium under the influence of magnetic field with wall slip condition. Veera Krishna and M.G.Reddy [28] discussed MHD free convective rotating flow of visco-elastic fluid past an infinite vertical oscillating plate. Veera Krishna and G.S.Reddy [29] discussed unsteady MHD convective flow of second grade fluid through a porous medium in a Rotating parallel plate channel with temperature dependent source.

In view of the above facts, in this chapter, an investigation of the heat and mass transfer on the flow of an oscillatory convective MHD viscous incompressible, radiating and electrically conducting second grade fluid in a vertical porous rotating channel in slip flow regime is carried out.

FORMULATION AND SOLUTION OF THE PROBLEM

Consider the flow of a viscous, incompressible and electrically conducting second grade fluid through a porous medium bounded by two infinite vertical insulated plates at d distance apart under the influence of uniform transverse magnetic field with magnetic flux density vector B_0 normal to the channel.

We introduce a Cartesian co-ordinate system with x-axis oriented vertically upward along the centreline of this channel and z-axis taken perpendicular to the planes of the plates which is the axis of the rotation and the entire system comprising of the channel and the fluid are rotating as a solid body about this axis with constant angular velocity Ω. A constant injection velocity w_0 is applied at the plate $z = -d/2$ and the same constant suction velocity, w_0, is applied at the plate $z = d/2$. The schematic diagram of the physical problem is shown in the Fig. 1.

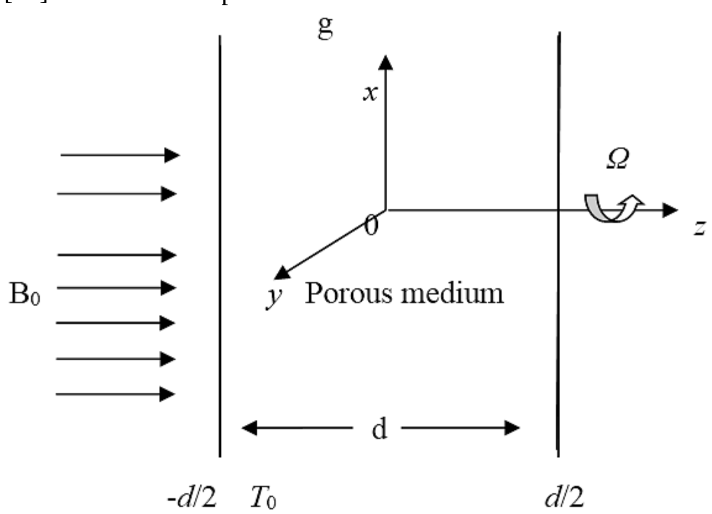

Figure 1. Physical Configuration of the Problem

Since the plates of the channel occupying the planes $z = \pm d/2$ are of infinite extent, all the physical quantities depend upon only on z and t only. Under the Boussinesq approximation the flow of the fluid through the porous medium in a rotating channel is governed by the following equation:

$$\frac{\partial w}{\partial z} = 0 \tag{2.1}$$

$$\frac{\partial u}{\partial t} - 2i\Omega v + w_0 \frac{\partial u}{\partial z} = -\frac{1}{\rho}\frac{\partial p}{\partial x} + \nu \frac{\partial^2 u}{\partial z^2} + \frac{\alpha_1}{\rho}\frac{\partial^3 u}{\partial z^2 \partial t} - \frac{\sigma B_0^2}{\rho} u - \frac{\nu}{k} u + g\beta T + g\beta_c C \tag{2.2}$$

$$\frac{\partial v}{\partial t} + 2i\Omega u + w_0 \frac{\partial v}{\partial z} = -\frac{1}{\rho}\frac{\partial p}{\partial y} + \nu \frac{\partial^2 v}{\partial z^2} + \frac{\alpha_1}{\rho}\frac{\partial^3 z}{\partial z^2 \partial t} - \frac{\sigma B_0^2}{\rho} v - \frac{\nu}{\kappa} v \tag{2.3}$$

$$\rho C_p \left(\frac{\partial T}{\partial t} + w_0 \frac{\partial T}{\partial z} \right) = K_1 \frac{\partial^2 T}{\partial z^2} - Q_0 T + Q_1 C - \frac{\partial q_1}{\partial z} \tag{2.4}$$

$$\frac{\partial C}{\partial t} + w_0 \frac{\partial C}{\partial z} = D \frac{\partial^2 T}{\partial z^2} - K_c C \tag{2.5}$$

The boundary conditions are

$$u = \frac{2 - f_1 L}{f_1}\frac{\partial u}{\partial z} = L\frac{\partial u}{\partial z}, v = \frac{2 - f_1 L}{f_1}\frac{\partial v}{\partial z} = L\frac{\partial v}{\partial z}, \; T = 0, C = 0, \quad \text{at} \quad z = -\frac{d}{2} \tag{2.6}$$

$$u = v = 0, \; T = T_0 \cos \omega t, C = C_0 \cos \omega t \quad \text{at} \quad z = \frac{d}{2} \tag{2.7}$$

Where, $L = \mu \left(\frac{\pi}{2p\rho} \right)^{1/2}$ is the mean free path which is constant for an incompressible fluid.

Following **Cogley et al [22]** the last term in the energy equation stand for radiative heat flux which is given by

$$\frac{\partial q_1}{\partial z} = 4\alpha^2 T \tag{2.8}$$

Where α is the mean variation absorption coefficient.

Introducing non-dimensional variables,

$$z^* = \frac{z}{d}, x^* = \frac{x}{d}, y^* = \frac{y}{d}, u^* = \frac{u}{d}, v^* = \frac{v}{d}, \theta = \frac{T}{T_0}, \; \phi = \frac{C}{C_0}, \; t^* = \frac{t\, w_0}{d}, \; p^* = \frac{p}{\rho w_0^2}, \omega^* = \frac{\omega d}{w_0}$$

Making use of non-dimensional variables, the equations (2.2), (2.3) and (2.4) reduces to (dropped asterisks)

$$\mathrm{Re}\left(\frac{\partial u}{\partial t} + \frac{\partial u}{\partial z} \right) - 2iRv = -\mathrm{Re}\frac{\partial p}{\partial x} + \frac{\partial^2 u}{\partial z^2} + S\frac{\partial^3 u}{\partial z^2 \partial t} - \left(M^2 + \frac{1}{K} \right) u + \mathrm{Gr}\,\theta + \mathrm{Gc}\phi \tag{2.9}$$

$$\mathrm{Re}\left(\frac{\partial v}{\partial t} + \frac{\partial v}{\partial z} \right) + 2iRu = -\mathrm{Re}\frac{\partial p}{\partial y} + \frac{\partial^2 v}{\partial z^2} + S\frac{\partial^3 v}{\partial z^2 \partial t} - \left(M^2 + \frac{1}{K} \right) v \tag{2.10}$$

$$\mathrm{Re}\,\mathrm{Pr}\left(\frac{\partial \theta}{\partial t} + \frac{\partial \theta}{\partial z} \right) = \frac{\partial^2 \theta}{\partial z^2} - \mathrm{Pr}\,\phi_1 \theta + \mathrm{Re}^2\,\mathrm{Pr}\, Q\phi - \mathrm{Pr}\, N^2 \theta \tag{2.11}$$

$$\mathrm{Sc}\,\mathrm{Re}\left(\frac{\partial\phi}{\partial t}+\frac{\partial\phi}{\partial z}\right)=\frac{\partial^2\phi}{\partial z^2}-\mathrm{Sc}\,\mathrm{Re}\,\mathrm{Kc}\,\phi \tag{2.12}$$

The corresponding boundary conditions in non dimensional form are

$$u=h\frac{\partial u}{\partial z},\ v=h\frac{\partial v}{\partial z},\ T=0 \quad \text{at} \quad z=-\frac{1}{2} \tag{2.13}$$

$$u=v=0,\ T=T_0\cos\omega t \quad \text{at} \quad z=\frac{1}{2} \tag{2.14}$$

Where, $\mathrm{Re}=\frac{w_0 d}{\nu}$ is Reynolds number, $R=\frac{\Omega d^2}{\nu}$ is the rotation parameter, $K=\frac{k}{d^2}$ is the permeability parameter, $\mathrm{Gr}=\frac{g\beta d^2 T_0}{\nu w_0}$ is the thermal Grashof number, $\mathrm{Gc}=\frac{g\beta_c d^2 C_0}{\nu w_0}$ is the mass Grashof number, $\mathrm{Pr}=\frac{\mu C_p}{K_1}$ is the Prandtl number, $\mathrm{Sc}=\frac{\nu}{D}$ is the Schmidt number, $\mathrm{Kc}=\frac{K_c d}{w_0}$ is the chemical reaction parameter, $N=\frac{2\alpha d}{\sqrt{K_1}}$ is the Radiation parameter, $\phi_1=\frac{Q_0 d^2}{\mu C_p}$ is the Heat absorption parameter, $Q=\frac{Q_1\nu C_0}{\rho C_p w_0^2 T_0}$ is the Radiation absorption number, $M^2=\frac{\sigma B_0^2 d^2}{\mu}$ is the Hartmann number and $S=\frac{\alpha_1}{\rho d^2}$ is the second grade fluid parameter.

Combining equations (2.9) and (2.10), let $q=u+iv$ and $\xi=x-iy$, we obtain

$$\mathrm{Re}\left(\frac{\partial q}{\partial t}+\frac{\partial q}{\partial z}\right)=-\mathrm{Re}\frac{\partial p}{\partial\xi}+\frac{\partial^2 q}{\partial z^2}+S\frac{\partial^3 q}{\partial z^2\partial t}-\left(M^2+2iR+\frac{1}{K}\right)q+\mathrm{Gr}\,\theta+\mathrm{Gc}\,\phi \tag{2.15}$$

We assume the flow under the influence of pressure gradient varying periodically with time,

$$-\frac{\partial p}{\partial\xi}=A\cos\omega t \tag{2.16}$$

The equation (2.16) is substituting in the equation (2.15) we obtain

$$\mathrm{Re}\left(\frac{\partial q}{\partial t}+\frac{\partial q}{\partial z}\right)=\mathrm{Re}\,A\cos\omega t+\frac{\partial^2 q}{\partial z^2}+S\frac{\partial^3 q}{\partial z^2\partial t}-\left(M^2+2iR+\frac{1}{K}\right)q+\mathrm{Gr}\,\theta+\mathrm{Gc}\,\phi \tag{2.17}$$

The corresponding boundary conditions are

$$q=h\frac{\partial q}{\partial z},\ \theta=0,\ \phi=0 \quad \text{at} \quad z=-\frac{1}{2} \tag{2.18}$$

$$q=0,\theta=\cos\omega t,\ \phi=\cos\omega t \quad \text{at} \quad z=\frac{1}{2} \tag{2.19}$$

In order to solve the equations (2.17), (2.11) and (2.12) with the boundary conditions (2.18) & (2.19) following **Choudary et al. [23]** we assume the solution of the form

$$q(z,t)=q_0(z)e^{i\omega t} \tag{2.20}$$

$$\theta(z,t)=\theta_0(z)e^{i\omega t} \tag{2.21}$$

$$\phi(z,t)=\phi_0(z)e^{i\omega t} \tag{2.22}$$

Substituting the equations (2.20), (2.21) and (2.22) in (2.17), (2.11) and (2.12) respectively, the resulting equations are,

We find the Skin Fraction τ_L at the left plate in terms of its amplitude and the phase angle as

$$\tau_L = \left(\frac{\partial q}{\partial z}\right)_{z=-\frac{1}{2}} = |q| \cos(\omega t + \gamma)$$

The rate of heat transfer (N_U) in terms of amplitude and the phase angle can be obtained as

$$Nu = \left(\frac{\partial T}{\partial z}\right)_{z=-\frac{1}{2}} = |r| \cos(\omega t + \psi)$$

Sherwood number:

The rate of mass transfer (Sh) in terms of amplitude and the phase angle can be obtained as

$$Sh = \left(\frac{\partial \phi}{\partial z}\right)_{z=-\frac{1}{2}} = |s| \cos(\omega t + \eta)$$

All the constants used above have been mentioned in the appendix.

RESULTS AND DISCUSSIONS

The effect of the Rotation number *R*, second grade fluid parameter *S* on the velocity profile shown by the Figs. 2. We noticed that the magnitude of velocity components *u* and *v* enhance with increasing *R* and *S* throughout the fluid region. Similar behaviour is observed for increasing thermal Grashof number Gr, permeability of the porous medium *K* and the amplitude of the pressure gradient *A* (Figs. 3).

The variations in the temperature profile are presented in the figs (4-7). It is observed from this Fig. 7 that the temperature profiles decrease with the increasing Reynolds number Re and the Prandtl number Pr. The similar behaviour is observed with increasing the radiation parameter *N* and Schmidt number Sc. The temperature profile is diminished with increasing chemical reaction parameter Kc, the radiation absorption parameter *Q*, the frequency of oscillation ω and it increases with the heat absorption parameter for $0 \le \phi_1 \le 1$ and decreases for $\phi_1 \ge 1$(Figs. 5-7).

A variation in the concentration profile is plotted in the Fig (8-9) and it is evident from the study of this figure that the amplitude of the concentration profile decreases with all the parameters Reynolds number Re, chemical reaction parameter Kc, Schmidt number Sc and the frequency of oscillation ω effecting the concentration equation.

The skin friction, Nusselt number and Sherwood number are evaluated analytically and tabulated in the tables. The amplitude and phase angle of the skin friction are shown in Table-1. The negative values in this table indicate that there is always a phase lag and this phase goes on increasing with increasing frequency of oscillation. We noticed that, the amplitude of stress $|q|$ and phase angle γ are enhanced with increasing the parameters *K*, *R*, *S*, Gr and Kc. Likewise the amplitude of the stress and the magnitude of the phase angle increases with Gc, Pr, *N*, *A*, *Q* and ϕ_1. The amplitude of stress $|q|$ reduces and phase angle γ increases with increasing *M*, *h* and ω. The reversal behaviour is observed with increasing Sc. From the table 2, we found that the amplitude $|r|$ and phase angle ψ of the Nusselt number increases with increasing Re, Pr, Sc and Kc. Also the amplitude of the Nusselt number decreases while phase angle ψ of the Nusselt number increases with increasing with N, ϕ_1 and ω. The opposite behaviour is observed with increasing *Q*.

Finally, From the table 3, we found that the amplitude $|s|$ and phase angle η of the Sherwood number decreases with increasing Re, Kc and ω. Also the amplitude of the Sherwood number decreases while phase angle ψ of the Sherwood number increases with increasing with Sc.

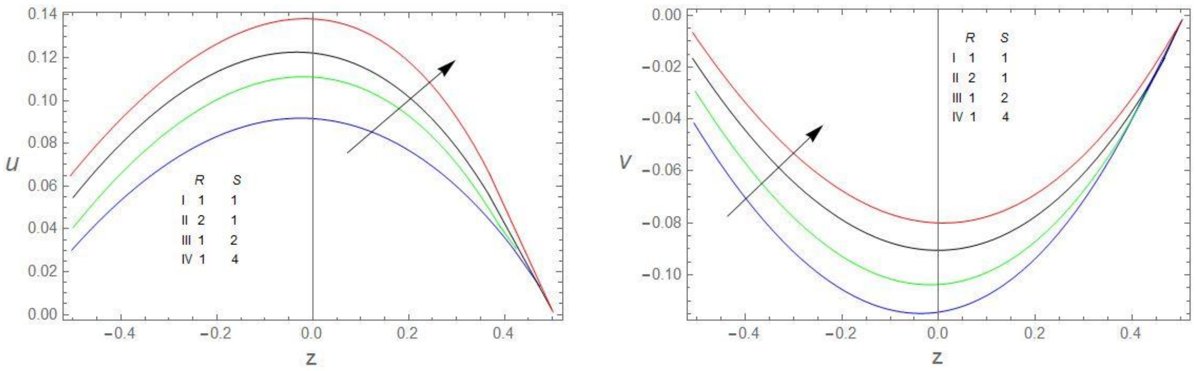

Figure 2. The velocity profiles for *u* and *v* against *R*, *m* and *S* with

$\mathrm{Gr}=3, M=0.5, \mathrm{Pr}=0.71, K=0.5, A=5, h=0.2, \phi_1=0.1, N=1, \omega=\pi/6, \mathrm{Gc}=5, \mathrm{Kc}=1, Q=1$

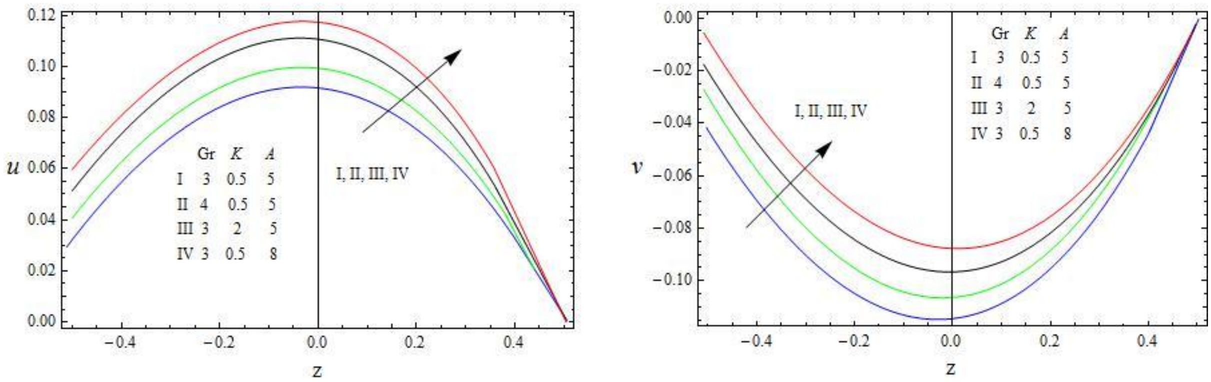

Figure 3. The velocity profiles for *u* and *v* against Gr, *K* and *A* with

$R=1, M=0.5, \mathrm{Pr}=0.71, S=1, h=0.2, \phi_1=0.1, N=1, \omega=\pi/6, \mathrm{Gc}=5, \mathrm{Kc}=1, Q=1$

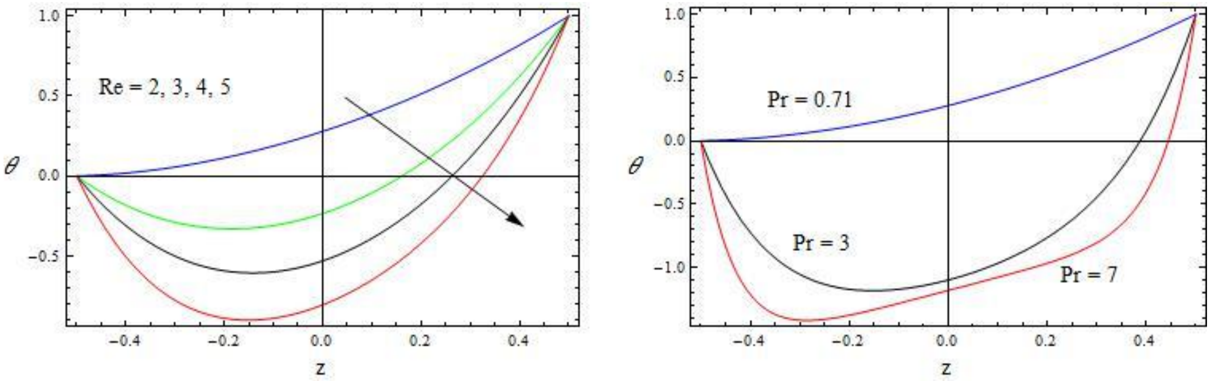

Figure 4. The Temperature profiles for θ against Re and Pr

$Q=0.5, \mathrm{Sc}=0.22, \mathrm{Kc}=1, \phi_1=0.1, \omega=\pi/6, N=1$

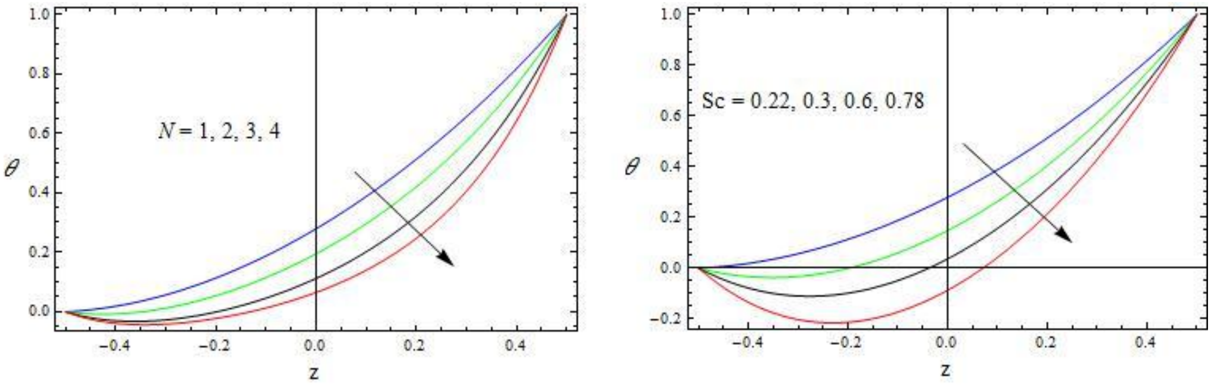

Figure 5. The Temperature profiles for θ against Re and Pr

$\mathrm{Re}=2, Q=0.5, \mathrm{Kc}=1, \phi_1=0.1, \omega=\pi/6, \mathrm{Pr}=0.71$

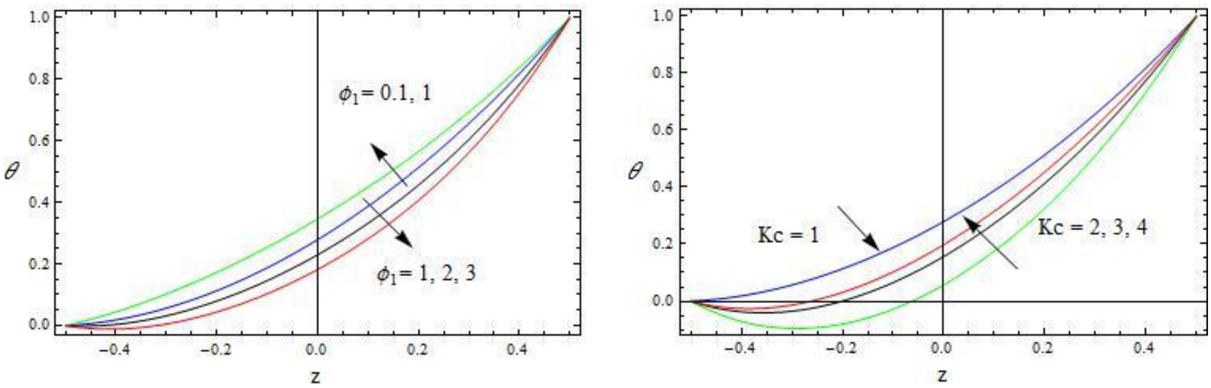

Figure 6. The Temperature profiles for θ against ϕ_1 and Kc

$\mathrm{Re}=2, Q=0.5, \mathrm{Sc}=0.22, \omega=\pi/6, \mathrm{Pr}=0.71, N=1$

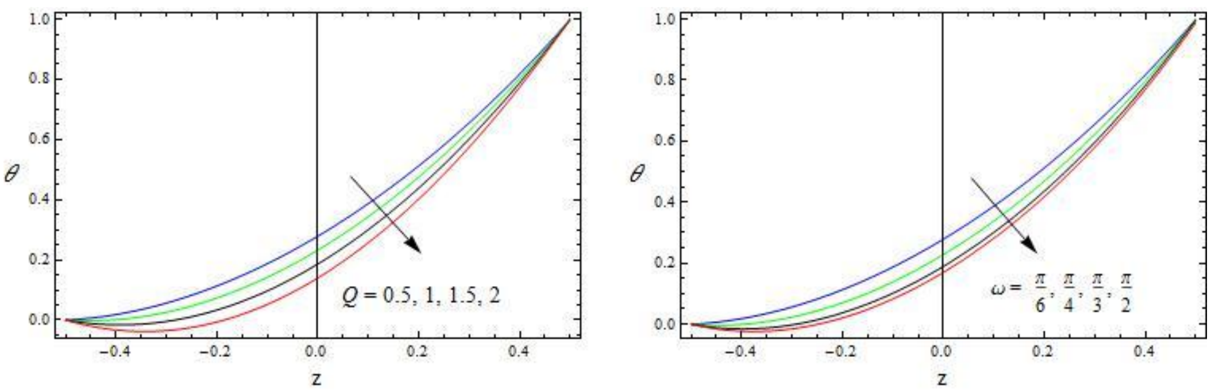

Figure 7. The Temperature profiles for θ against Q and ω

$\mathrm{Re}=2, \mathrm{Sc}=0.22, \mathrm{Kc}=1, \phi_1=0.1, \mathrm{Pr}=0.71, N=1$

International Journal of Applied Engineering Research ISSN 0973-4562 Volume 13, Number 7 (2018) pp. 4652-4662

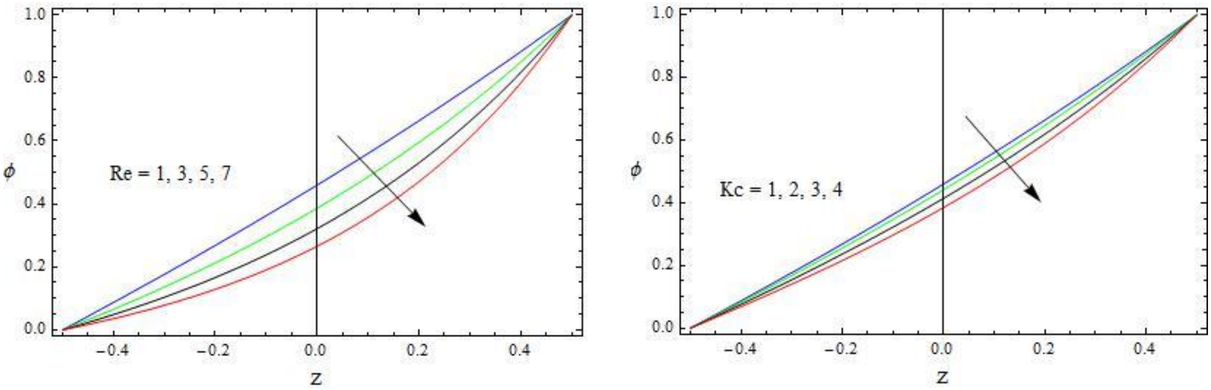

Figure 8. The Concentration profiles for ϕ against Re and Kc with

$\mathrm{Sc} = 0.22, \omega = \pi / 6$

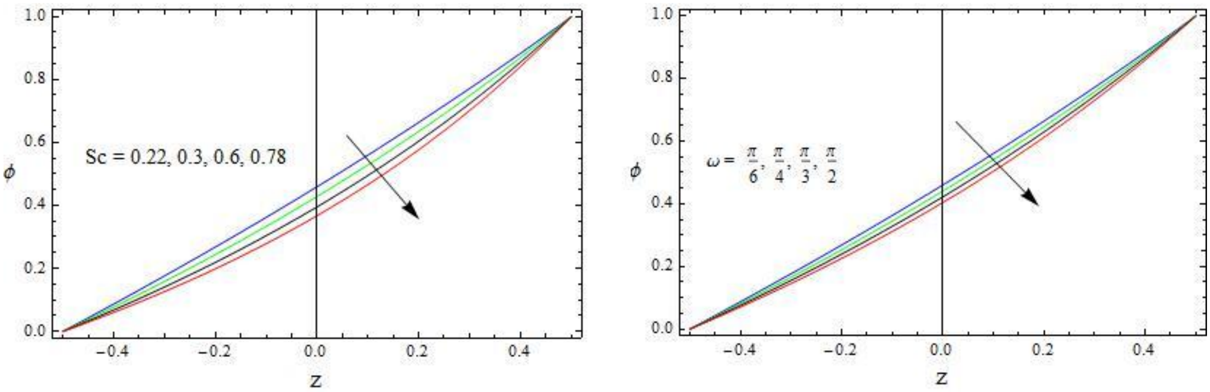

Figure 9. The Concentration profiles for ϕ against Sc and ω with $\mathrm{Sc} = 0.22, \omega = \pi / 6$

Table 1: Amplitude and Phase angle of Skin friction for $\mathrm{Re} = 0.5,\ t = 0.1$

M	***K***	***R***	***S***	**Gr**	**Gc**	**Pr**	***N***	***A***	***h***	ω	***Q***	**Kc**	**Sc**	ϕ_1	**Amplitude** $\lvert q \rvert$	**Phase angle** γ
0.5	**0.5**	**1**	**1**	**3**	**5**	**0.71**	**1**	**5**	**0.2**	$\pi / 6$	**1**	**1**	**0.22**	**1**	2.41838	0.283666
1															2.08139	0.493308
1.5															1.84239	0.912284
	1														4.12001	0.361881
	2														4.74557	0.546996
		1.5													2.60643	0.702051
		2													2.93479	0.953428
			2												3.56638	0.449328
			3												4.52993	0.530073
				4											6.10330	1.22620
				5											10.9613	1.40566
					6										2.76792	-0.494756

					7										4.17485	-0.913639
						3									3.40990	-1.28415
						7									4.98979	-2.16613
							2								3.96028	-0.852479
							3								5.34219	-0.973996
								7							3.52703	-0.332539
								9							5.26923	-0.601007
									0.3						2.36727	0.406581
									0.4						2.33804	0.502298
										$\pi/4$					1.72973	1.35433
										$\pi/3$					0.16745	1.51188
											2				17.5185	-1.52284
											3				34.5524	-2.45473
												2			3.39423	0.44864
												3			4.83245	0.60745
													0.3		5.70465	0.16883
													0.6		28.5275	0.09419
														1.5	7.44764	-0.70043
														2	9.74770	-0.89663

Table 2: Amplitude and Phase angle of Nusselt number for $t = 0.1$

Re	**Pr**	**N**	ϕ_1	**Sc**	**Kc**	***Q***	ω	**Amplitude** $\lvert r \rvert$	**Phase angle** ψ
2	**0.71**	**1**	**0.2**	**0.22**	**0.2**	**1**	$\pi/6$	4.31112	0.538747
3								12.6750	1.230090
4								16.1478	1.527450
	3							21.6871	1.405730
	7							45.0290	1.536470
		2						4.22257	1.466980
		3						3.93830	1.491090
			0.5					2.79348	0.667940
			1					2.33856	1.104290
				0.3				5.57300	0.627978
				0.6				16.0440	1.447030
					0.4			5.36079	1.377640
					0.6			5.82016	1.541990
						2		7.58466	0.355346
						3		10.9587	0.283540
							$\pi/4$	4.27767	0.853784
							$\pi/3$	4.15536	1.011080

Table 3: Amplitude and Phase angle of Sherwood number for $t = 0.1$

Re	**Sc**	**Kc**	ω	**Amplitude** $\lvert s \rvert$	**Phase angle** η
2	**0.22**	**0.2**	$\pi/6$	0.740534	1.55564
3				0.634072	-1.55232
4				0.541233	-1.55138
	0.3			0.661697	1.56853
	0.6			0.427695	1.62798
		0.4		0.690418	1.55465
		0.6		0.644864	1.55373
			$\pi/4$	0.740284	1.54805
			$\pi/3$	0.739937	1.54045

CONCLUSIONS

The resultant velocity enhance with increasing *R*, *S*, Gr, *K* and *A* throughout the fluid region. The velocity profile is diminished with the increasing ϕ_1, *h*, ω, *M*, Pr and *N*. The resultant velocity enhances with increasing Gc and continuously reduces with increasing Kc and *Q* in the entire fluid region. The temperature profiles decrease with the increasing Re, Pr, *N* and Sc. The temperature profile is diminished with increasing Kc, and ω. The concentration profile decreases with all Re, Kc, Sc and ω. The amplitude and phase angle of frictional force are enhanced with increasing the parameters *K*, *R*, *S*, Gr and Kc. The amplitude and phase angle of the Nusselt number increases with increasing Re, Pr, Sc and Kc. Also the amplitude of the Nusselt number decreases while phase angle of the Nusselt number increases with increasing with N. The amplitude and phase angle of the Sherwood number decreases with increasing Re, Kc and ω.

REFERENCES

[1]. A. Bejan, K.R. Khair, Heat and mass transfer by natural convection in a porous medium, Int. J. Heat Mass Transf. 28 (1985) 909-918.

[2]. F.C. Lai, Coupled heat and mass transfer by mixed convection from a vertical plate in a saturated porous medium, Int. Commun. Heat Mass Transf. 18 (1991) 93-106.

[3]. A.R. Bestman, Natural convection boundary layer with suction and mass transfer in a porous medium, Int. J. Energy Res. 14 (1990) 389-396.

[4]. V.M. Soundalgekar, Effects of mass transfer on flow past a uniformly accelerated vertical plate, Lett. Heat Mass Transf. 9 (1982) 65-72.

[5]. A.K. Singh, J. Singh, Mass transfer effects on the flow past an accelerated vertical plate with constant heat flux, Astrophys. Sp. Sci. 97 (1983) 57-61.

[6]. K.N. Mehta, K.N. Rao, Buoyancy-induced flow of non-Newtonian fluids in a porous medium past a vertical plate with nonuniform surface heat flux, Int. J. Eng. Sci. 32 (1994) 297-302.

[7]. Yue-Tzu Yang, S. Wang, Free convection heat transfer of non-Newtonian over axisymmetric and two-dimensional bodies of arbitrary shape embedded in a fluid- saturated porous medium, Int. J. Heat Mass Transf. 39 (1996) 203.

[8]. H.T. Chen, C.K. Chen, Free convection of non-Newtonian fluids along a vertical plate embedded in a porous medium, ASME J. Heat Transf. 110 (1988) 257e260.

[9]. R.Y. Jumah, A.S. Mujumdar, Free convection heat and mass transfer of nonNewtonian power-law fluids with yield stress from a vertical flat plate in a saturated porous media, Int. Commun. Heat Mass Transf. 27 (2000) 485-494.

[10]. S. Abel, P.H. Veena, Visco-elastic fluid flow and heat transfer in a porous medium over a stretching sheet, Int. J. Non-Linear Mech. 33 (1998) 531-540.

[11]. A. Raptis, A.K. Singh, MHD free convection flow past an accelerated vertical plate, Int. Comm. Heat Mass Transf. 10 (1983) 313-321.

[12]. T. Gul, S. Islam, R.A. Shah, I. Khan, S. Shafie, Heat transfer analysis of MHD thin film flow of an unsteady second grade fluid past a vertical oscillating belt, PLoS One 9 (11) (2014) e103843.

[13]. M. Abdulhameed, I. Khan, S. Shafie, Closed form solutions for unsteady MHD flow in a porous medium with wall transpiration, J. Porous Media 16 (9) (2013) 795-809.

[14]. T.K. Aldoss, M.A. Al-Nimr, M.A. Jarrah, B.J. Al-Shaer, Magnetohydrodynamic mixed convection from a vertical plate embedded in a porous medium, Numer. Heat Transf. 28 (1995) 635.

[15]. A.J. Chamkha, Unsteady MHD convective heat and mass transfer past a semiinfinite vertical permeable moving plate with heat absorption, Int. J. Eng. Sci. 42 (2004) 217-230.

[16]. M.G. Reddy, Radiation effects on MHD natural convection flow along a vertical cylinder embedded in a porous medium with variable surface temperature and concentration, Front. Heat Mass Transf. (FHMT) 5 (2014) 4.

[17]. B.I. Olajuwon, J.I. Oahimire, M. Ferdow, Effect of thermal radiation and Hall current on heat and mass transfer of unsteady MHD flow of a viscoelastic micropolar fluid through a porous medium, Eng. Sci. Technol. Int. J. (2014), http://dx.doi.org/10.1016/j.jestch.2014.05.004.

[18]. A. Khan, I. IKhan, F. Ali, S. Shafie, Effects of wall shear stress MHD conjugate flow over an inclined plate in a porous medium with ramped wall temperature, Math. Probl. Eng. (2014) 15. Article ID 861708.

[19]. A. Hussnan, Z. Ismail, I. Khan, S. Shafie, Unsteady MHD free convection flow in a porous medium with constant mass diffusion and Newtonian heating, Eur. Phys. J. e Plus 129 (2014) 46.

[20]. Samiulhaq, A. Sohail, D. Vieru, I. Khan, S. Shafie, Unsteady magnetohydrodynamic free convection flow of a second grade fluid in a porous medium with ramped wall temperature, PLoS One 9 (5) (2014) e88766.

[21]. M. Mirzaei nejad, K. Javaherdeh, Numerical simulation of power-law fluids flow and heat transfer in a parallel-plate channel with transverse rectangular cavities, Case Stud. Therm. Eng. 3 (2014) 68-78.

[22]. M. Donisete de Campos, E.C. Romao, L.F. Mendes de Moura, A ~ finite-difference method of high-order accuracy for the solution of transient nonlinear diffusiveeconvective problem in three dimensions, Case Stud. Therm. Eng. 3 (2014) 43-50.

[23]. M. Hatami, D.D. Ganji, Natural convection of sodium alginate (SA) nonNewtonian nanofluid flow between two vertical flat plates by analytical and numerical methods, Case Stud. Therm. Eng. 2 (2014) 14-22.

[24]. M.A.Y. Bakier, Flow in open C-shaped cavities: how far does the change in boundaries affect nanofluid? Eng. Sci. Technol. Int. J. 17 (2014) 116-130.

[25]. M.H. Mohamed, A.M. Ali, A.A. Hafiz, CFD analysis for H-rotor Darrieus turbine as a low speed wind energy converter, Eng. Sci.Technol. Int. J. (2014), http:// dx.doi.org/10.1016/j.jestch.2014.08.002.

[26]. VeeraKrishna.M and B.V.Swarnalathamma (2016) Convective Heat and Mass Transfer on MHD Peristaltic Flow of Williamson Fluid with the Effect of Inclined Magnetic Field," AIP Conference Proceedings 1728:020461

doi: http://dx.doi.org/10.1063/1.4946512

[27]. Swarnalathamma. B. V. and M. Veera Krishna (2016) Peristaltic hemodynamic flow of couple stress fluid through a porous medium under the influence of magnetic field with slip effect AIP Conference Proceedings 1728:020603

doi: http://dx.doi.org/10.1063/1.4946654

[28]. VeeraKrishna.M and M.Gangadhar Reddy (2016) MHD free convective rotating flow of Visco-elastic fluid past an infinite vertical oscillating porous plate with chemical reaction IOP Conf. Series: Materials Science and Engineering 149:012217

doi: http://dx.doi.org/10.1088/1757-899X/149/1/012217.

[29]. VeeraKrishna/M and G.Subba Reddy (2016) Unsteady MHD convective flow of Second grade fluid through a porous medium in a Rotating parallel plate channel with temperature dependent source IOP Conf. Series: Materials Science and Engineering, 149:012216 doi**:** http://dx.doi.org/10.1088/1757-899X/149/1/012216.